❒       3496

# A metamaterial inspired multi band antenna using complementary split ring resonator for wireless applications

**Harshavardhan Reddy[1,2], Rajendra R. Patil[1]**

[1]Department of Electronics and Communication Engineering, GSSS Institute of Engineering and Technology for Women–Mysuru, Affiliated to Visvesvaraya Technological University, Belagavi, Karnataka, India
[2]Department of Electronics and Communication Engineering, Faculty of Engineering and Technology, Sharnbasva University, Kalaburagi, India

## Article Info

## ABSTRACT

This research introduces a new printed metamaterial antenna with triple and quad bands for wireless applications. The suggested antenna is constructed of FR4 material, with two slots created in the radiating element. In addition, a circular complementary split ring resonator (C-CSRR), is carved from the ground plane. HFSS simulation software is being put into use to design, model, and measure the suggested antenna parameters in a real-world environment. The measured results indicate that an antenna with C-CSRR behind the radiating patch resonates at three distinct frequencies, including 3.5 GHz, 7.5 GHz, and 8.2 GHz, and an antenna with C-CSRR and slots on the radiating patch resonates at four different frequencies, including 3.5 GHz, 7.5 GHz, 8.8 GHz, and 9.32 GHz. An antenna without complementary split ring resonator (CSRR), or a conventional antenna, resonates at 9.6 GHz. The metamaterial antenna results in a 65% diminution in antenna size in contrast to a regular microstrip antenna. The simulated outcome demonstrates that the suggested metamaterial antenna's peak gain is around 6 dB to 8 dB and it has a resonance frequency for C-band applications, including weather radar systems and 5G applications.

*Corresponding Author:*

Harshavardhan Reddy
Department of Electronics and Communication Engineering, Faculty of Engineering and Technology
Sharnbasva University
Kalaburagi 585102, Karnataka, India
Email: harshareddy86@gmail.com

## 1. INTRODUCTION

The rapid growth and popularity of wireless communication in recent years have increased the need for a miniaturized multiband antenna to cut down on the volume of antennas used in single devise. The microstrip patch is the most demanding antenna on the bases of its uses, and it has benefits like minimal manufacturing cost and light weight in addition it works across a broad frequency range. Additionally, radiating patches can be made in a number of forms, including elliptical, triangular, square, rectangular, and more. When operating with a single ended signal, radio frequency equipment frequently uses microstrip antennas. Recent microwave designs have utilized a wide range of metamaterials in conjunction with this, as both a top layer or as the substrate. Microstrip antennas are frequently used in wireless devices in contemporary wireless communication networks. As a result, lowering the size of the complete communication system has become dependent on the antenna's ability to be miniaturized. Research by Veselago [1] wrote a scientific study on the notion of metamaterial in 1968. Usually created artificially, these metamaterials are composite structures made of periodic metallic patterns deposited on dielectric substrates.

In the context of microwave applications, metamaterials have recently received a lot of research attention. Several works have addressed towards the performance improvement of antennas in the microwave range of frequencies.

A small tri band antenna with hexa-complementary split-ring resonators (HCSRRs) is designed for 4G communication [2]. Bands have been adjusted such that it covers the operating bands of wireless local area networks (WLAN), WiMAX, and Wi-Fi by carefully selecting the ideal dimensions and location of the complementary split ring resonator (CSRR). An article describes the use of hexagonal CSRR slots in a compact multiband printed monopole antenna. In order to assess the small antenna's multiband capabilities, the pass band properties of HCSRR are thoroughly analyzed [3]. A modified complementary split ring resonator (SRR) is etched on the ground layer to create permeable bands that could support several resonant frequencies in a single gadget [4], the antenna's bandwidth can be increased by splitting in the outer hexagonal ring of a hexagonal CSRR [5]. Two different types of 5G indoor distributed antenna systems (IDAS) based on metamaterial antennas are suggested [6], where both antennas function in the 3.5 GHz–6 GHz 5G range. The radiating configuration of the antenna is made up of two CSRR unit-cells carved on the highest layer, in addition to a combination of rectangular and triangular patches.

The trapezoidal segment of the suggested antenna is a radiant patch with a loaded triangular CSRR and a partial ground plane [7]. Lower and higher frequencies are produced by the trapezoidal radiating patch, whereas loading the TCSRR structure yields the two other resonance frequencies. On the front side of the basic rectangular patch antenna, the patch line feeding element's sides are lined with the CSRR metamaterial structure. A CSRR is installed as metamaterials and can be employed to boost antenna array isolation. CSRRs are small resonating elements that produce an excellent quality factor at microwave frequencies [8]. An impedance bandwidth (IBW) of 5.8–15 GHz (98.63%) was attained by a metamaterial-inspired ultra wide band-multiple input multiple output (MIMO) fractal antenna by lowering the mutual coupling between the two radiating components to less than -25 dB [9]. On the exterior side of the basic rectangular patch antenna, the CSRR is placed along the edges of the micro patch line feeding element. The redesigned split-ring resonator (SRR) is located on the rear side of the suggested antenna. At the frequency of resonance (fr)=2.4 GHz, this antenna produced the best results, with a return loss of -46.58 dB, a bandwidth of 574 MHz, and a gain of 3.23 dBi [10].

In order to obtain octa band properties for wireless standards, an article [11] describes a multiband antenna that uses slots, a quasi-complementary split-ring resonator (Q-CSRR), and a metamaterial SRR. By putting the SRR and CSRR cells and using the slot technique in the radiating section component, multiband characteristics are achieved. A different study, motivated by metamaterials, suggests a novel antenna with a bottom patch and shunt fractal inductor on tiny cylindrical creating a dual-band antenna. Three composite meander line-type unit cells make up the conformal antenna. In order to enhance the operational bandwidth in the initial band, namely at 2.45 GHz, a large inductance shunt fractal inductor is suggested [12] for improved impedance matching, an identical patch with a gap along the down side is also utilized. Two weave line unit cells are loaded onto the patch as intrinsic elements that create the second band at 3.5 GHz. It has been suggested to build a millimeter-wave single-layered MIMO antenna that functions at 28 GHz and is equipped with microscopic planar-patterned metamaterial structures [13]. In addition to a near-zero refractive index (NZRI) property, a unit cell with a split square and hexagonal shape combination is built and examined with a variety of viable near-zero index (NZI) permittivity and permeability values. The properties of the metamaterial were studied from material wave propagation in the two principal paths at the y-axis and x-axis. Its NZRI, mu-near-zero (MNZ), and epsilon-near-zero (ENZ) are displayed, and its y-axis wave propagation bandwidth exceeds 6 GHz.

The development and evaluation of a split ring metamaterial broad-band patch antenna are presented in this study [14]. Sub-wavelength modes are produced in the patch antenna due to the unique and innovative way in which the SRR metamaterial structures are incorporated. A patch cavity and an antenna with good performance qualities and a broad bandwidth are developed. A rectangular microstrip patch antenna with a resonance frequency of 5.2 GHz and an IBW of 70 MHz serves as the reference antenna, in order to enhance the patch antenna's bandwidth, the SRR is initially created based on the reference patch antenna. Wide-scale steering range is made possible by the ground structure loaded with CSRR; it also considerably reduces the price of a phased-array system required to meet wireless communications standards. An examination of the CSRR structure's parameter extraction is conducted to examine how the loading metamaterial affects the antenna's radiation pattern [15]. The construction and inspection of a four-band fractal square monopole with a complementing SRR-backed ground plane are suggested in this article [16]. The monopole antenna's increased bandwidth is due to its metamaterial property. The four microwave frequency bands that the antenna operates in are 4.43–4.57 GHz, 5.80–6 GHz, 6.97–7.36 GHz, or C-band, and 7.89–8.18 GHz, or X band. Basic ideas for patch antennas influenced by metamaterials have been documented in [17]–[21].

A novel ground plane complementary slotted split ring resonator (CSlSRR) is created [22]. With the inset feed, CP is produced by semi-circular arcs with truncated edges. The CSlSRR aids in the antenna's

3498  ❐

miniaturization and bandwidth improvement. The design succeeds in a 61% decrease in size. The designed antenna has its optimum gain of 2.476 dBi at 2.75 GHz, an axial ratio bandwidth (ARBW) of 4.07%, and an IBW of 12.3%. An antenna with a broad bandwidth feature is needed to provide these 5G capabilities, however their constructions are too huge. However, one of the most intriguing and widely used designs is the microstrip patch antenna because of its tiny size, airborne weight, affordability, and it's simple to integrate and manufacture [22]–[25].

## 2. ANTENNA DESIGN

The suggested antenna makes use of a regular rectangular patch which resonate at 10 GHz. The proposed traditional microstrip antenna's profile is shown in Figure 1, wherein minimal manufacturing cost FR4-Epoxy dielectric material with its dielectric constant ($\varepsilon_r$) of 4.4 and thickness (h) of 1.6 mm is selected. The parameters need to be computed are as below [14];
Width (W): to calculate the width of the patch, use (1):

$$W = \frac{C_0}{2f_r}\sqrt{\frac{2}{\varepsilon_r+1}} \tag{1}$$

Here, $W$ is width of the patch; $C_0$ is speed of light; and $\varepsilon_r$ is the value of dielectric substrate.
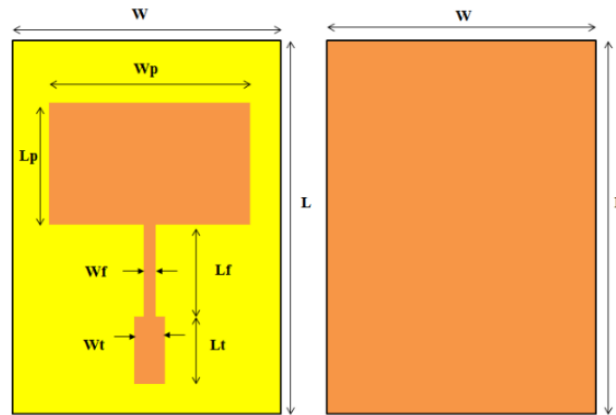


Figure 1. Conventional antenna radiating and ground plane

Effective refractive index: this parameter is one of the important considerations while structuring of a microstrip patch antenna. A portion of the radiation that exits the patch and heads toward the ground (fringing) passes through the substrate in addition to the air. Because the properties of dielectric substrates and the open air differ, we must compute the effective dielectric constant by taking this into consideration. The effective dielectric constant ($\varepsilon_{r\text{eff}}$) can be calculated using (2):

$$\varepsilon_{reff} = \frac{\varepsilon_r+1}{2} + \frac{\varepsilon_r-1}{2}\left[1 + 12\frac{h}{W}\right]^{1/2} \tag{2}$$

Length: the antenna's size increases electrically due to fringe by a factor of ($\Delta L$). In order to calculate the actual length increase ($\Delta L$) of the patch, (3) should be employed:

$$\frac{\Delta L}{h} = 0.412\frac{(\varepsilon_{reff}+0.3)\left(\frac{W}{h}+0.264\right)}{(\varepsilon_{reff}-0.258)\left(\frac{W}{h}+0.8\right)} \tag{3}$$

where, $h$ is height of the substrate.
Now, using (4), determine the length (L) of the patch:

$$L = \frac{C_0}{2f_r\sqrt{\varepsilon_{reff}}} - 2\Delta L \tag{4}$$

Length ($L_g$) and width ($W_g$) of ground plane: currently, we know the patch's dimensions. The substrate and the ground plane have the identical measurements. Make use the following formulas to determine a ground plane's $L_g$ and $W_g$:

$$L_g = 6h + L \; and \; W_g = 6h + W \tag{5}$$

The traditional MSA is constructed for 10 GHz and has dimensions L and W radiating parts that are excited by a basic 50 Ω microstrip feed with dimensions $L_p$ and $W_p$. A quarter wave length transformer with dimensions $L_f$ and $W_f$ is used to match their impedance. Table 1 has a list of all the dimensions along with the $L_g$ and $W_g$ of the antenna's ground plane, which are computed as $L_g=6h+L$ and $W_g=6h+W$.

Table 1. Various measurements of the patch, the underneath ground plane and CCSRR

| Label | Size (mm) | Label | Size (mm) |
|-------|-----------|-------|-----------|
| W | 23.3 | W1 | 0.4 |
| L | 30.19 | W2 | 0.2 |
| $W_f$ | 3.059 | L1 | 5 |
| $L_f$ | 6.85 | r1 | 2.4 |
| $W_t$ | 0.723 | r2 | 3 |
| $L_f$ | 4.313 | S1 | 0.3 |
| $W_p$ | 9.13 | S2 | 0.3 |
| $L_p$ | 6.43 | g | 0.3 |

The intended construction's evolution is shown in Figure 1. A steady ground and a rectangle microstrip line patch make up layout I. To achieve the necessary resonance frequency of 10 GHz, this is regular microstrip patch antenna.

This section addresses the resonance frequency of the CSRR making use of an LC parallel tank circuit [10]. One of the essential CSRR properties is the slit gap. If the slit is eliminated, CSRR will not produce a particular resonance frequency. SRRs and CSRRs function as an analogous LC circuit, as shown by the theory and mathematical analysis of these circuits.

Figure 2 depicts the CSRR structure and its inherent equivalent circuit model. This analogous circuit is made up of two parallel inductors, each of which is represented by $L_0/2$ and connects the disc to ground, as well as a capacitance, CCSRR, that is made up of a disc with a radius of $r_0$-c/2 that is encircled by a ground plane.
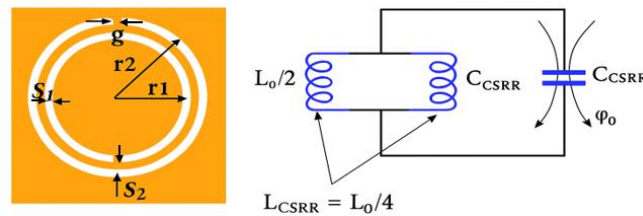


Figure 2. LC circuit with its identical CSRR structure

The LC tank circuit diagram shown in Figure 2 determines the circular CSRR's resonance frequency. The circular complementary split ring resonator (C-CSRR's) slit gap is crucial for generating pass band behavior. The inductance effect ($L_{CSRR}$) is caused by the slit along the slot, and the capacitance effect ($C_{CSRR}$) is caused by the slot along the slit. The CSRR inductance ($L_{CSRR}$) is caused by the copper strip within the slots, whereas the capacitance ($C_{CSRR}$) is caused by the gap across the copper strips. SRR and CSRR are regulated by the same expression when using babinet principle.

Therefore, the CCSRR resonance frequency is calculated by:

$$f_{CSRR} = \frac{1}{2\pi\sqrt{L_{CSRR}C_{CSRR}}} \tag{6}$$

where,

$$C_{CSRR} = \frac{N-1}{2}[2L - (2N-1)(W+S)]C_0 \tag{7}$$

$$C_0 = \varepsilon_0 \frac{K(\sqrt{1-K^2})}{K(k)} \text{ and } k = \frac{\frac{S}{2}}{W+\frac{S}{2}} \tag{8}$$

$$L_{CSRR} = 4\mu0[L - (N-1)(S+W)]\left[ln\left(\frac{0.98}{\rho}\right) + 1.84\rho\right] \tag{9}$$

$$\rho = \frac{(N-1)(S+W)}{1-(N-1)(W+S)} \tag{10}$$

Here, N is the number of circular CSRR slots, the radius R of the CSRR *(L)*, a slot width of the CSRR *(W)*=0.3 mm, the distance between the CSRR slots *(S)*=0.3 mm and K is the first order elliptic integral *K(k)*. The appearance of the ratio in (8) is a standard form in quasi-static capacitance calculations, particularly in conformal mapping techniques used for planar transmission lines or resonator structures. This elliptic integral is dimensionless and depends only on the modulus k, which, in this antenna design, is derived from geometrical parameters (slot width W and spacing S). To determine the resonance frequency of CSRR owing to inductance ($L_{CSRR}$) and capacitance ($C_{CSRR}$) values, a MATLAB software analyzes these exact design formulae. 3.56 GHz is the resonance frequency of the CSRR with N=2 slots.

Figure 3 shows the proposed antennas. As illustrated in Figure 3(a), the investigation is carried out by engraving a circular CSRR in the ground plane. The CSRR is etched with an outermost radius of 3 mm from the ground plane at a point of x=0 mm along y=0 mm. The experiment is continued for different values of r2 i.e., radius of outer circle represented by R. The radius values of R, are chosen to demonstrate the effective value of R for which the outcome of the antenna is optimum. Figure 3(b) illustrates the final suggested antenna design. Here the slots on the patch are made to enhance the bandwidth of the antenna. The slot is chosen from the best of different trials taken for different length and width of the slot.
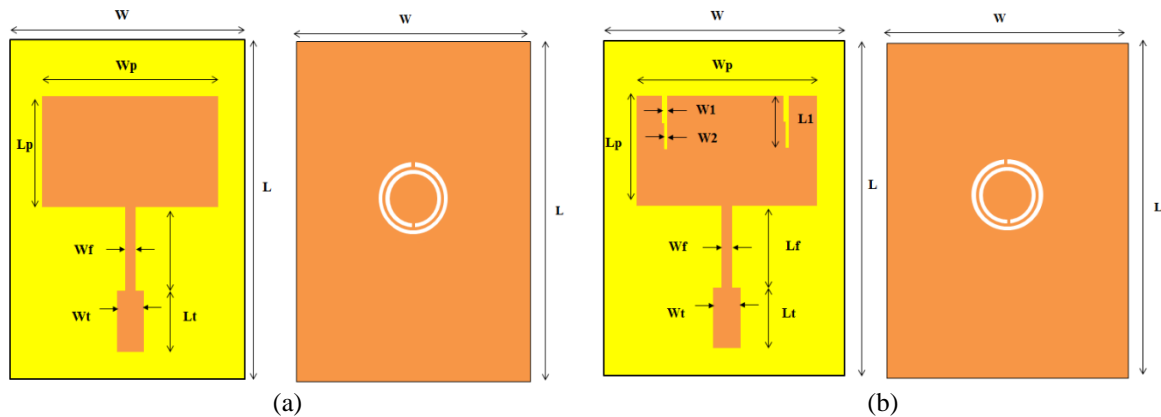


Figure 3. Proposed antennas; (a) antenna with circular CSRR on ground plane and (b) antenna with circular CSRR on ground plane with slots on patch

The CSRR unit cell is engraved onto the ground plane to keep the antenna's size as compact as possible. The CSRR reacts with the electric field and creates an actual negative permittivity at its resonance frequency. By engraving CSRR on the ground plane, it is simple to excite these resonators, shift the antenna's resonating frequency to the left, and effectively minimize the antenna's size by virtue of the many resonating locations. The circular CSRR antenna on the ground plane is therefore resonating over three separate frequency locations. The circular CSRR's parameters are S1=0.3 mm, S2=0.3 mm, g=0.3 mm, r2=3 mm, and r1=2.4 mm. The extended geometry of the CSRR with variables and its analogous LC circuit are shown in Figure 2.

## 3. RESULTS AND DISCUSSION

ANSYS HFSS simulation software version 15 is used for all the simulations. All of the proposed antenna's properties, including radiation pattern, return loss, bandwidth and size reduction were investigated through simulation and confirmed using a scalar network analyzer. It is evident from the data that by engraving a circular CSRR on the ground and including a slot on the radiating patch, the resonant frequency

was greatly reduced, which led to a decrease in size. Because of the circular CSRR, the antennas' bandwidths have improved. Additionally, each and every antenna that has been demonstrated has many resonances.

The Figure 4 demonstrates the simulated return loss for various value of r2 (R), varied in between 2.5 mm to 4 mm, the gap between the two rings (S1 and S2) is kept constant accordingly the value of r1 changes w.r.t change in r2 (R). Here it is observed that the ideal return loss for the desired application is obtained at R=3 mm, and the antenna with 3 mm radius circular CSRR is etched with slot on radiating element to increase the bandwidth and resonate at desired frequencies.
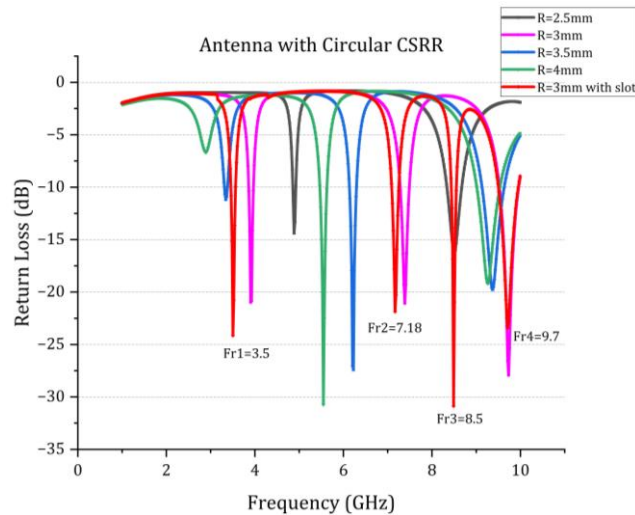


Figure 4. Return loss of antennas with different ranges of R

The Figure 5 demonstrates the proposed antenna's multiple resonance frequencies (Fr1=3.5 GHz, Fr2=7.5 GHz, and Fr3=8.2 GHz) and total bandwidth of 10.14% (2.84%+3.16%+4.14%) result in a size reduction of 65% to 24%. The circular CSRR on the ground plane, which is mainly responsible for the increased frequency bandwidth, also helps to lower the antenna's resonance frequency.
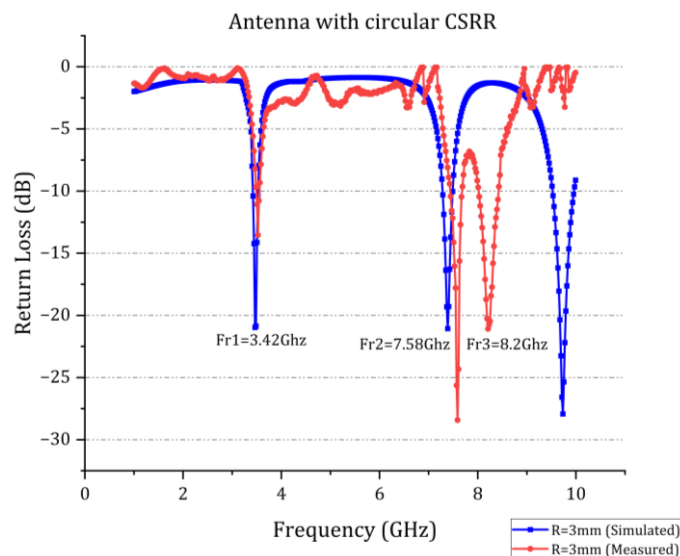


Figure 5. Return loss of antenna with circular CSRR

As mentioned, Figure 3(b) illustrates the final suggested antenna design. It has a circular CSRR on the ground plane and slots on the radiating plane, and it exhibits active response in multiple frequencies with centers at Fr4=3.5 GHz, Fr5=7.5 GHz, Fr6=8.8 GHz, and Fr7=9.3 GHz. These frequencies have return losses of -13.23 dB, -16.32.1 dB, -30.26.0 dB, and -36.75 dB respectively, as shown in Figure 6.
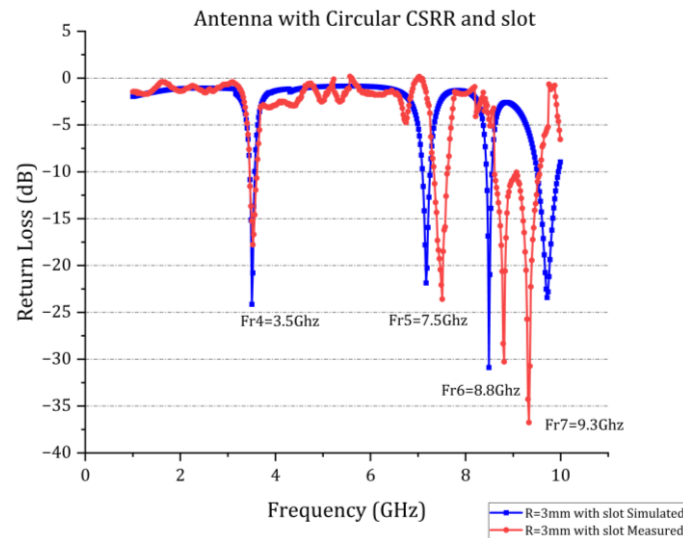
Figure 6. Return loss of antenna with circular CSRR and slots

The projected multiband antenna's simulated gain is seen in the Figure 7, i.e., 6.24 dB, 6.33 dB, and 8.01 dB for frequencies 3.5 GHz, 7.5 GHz, and 9.7 GHz, shown in Figures 7(a)-(c) respectively. Sometimes the gain pattern is also known as the gain at function direction plot. With the help of the HFSS application, the gain is shown in a 3D polar plot. The gain of the antenna enhanced and examined in contrast to other designs by incorporating a reflector, DGS, and parasitic elements.
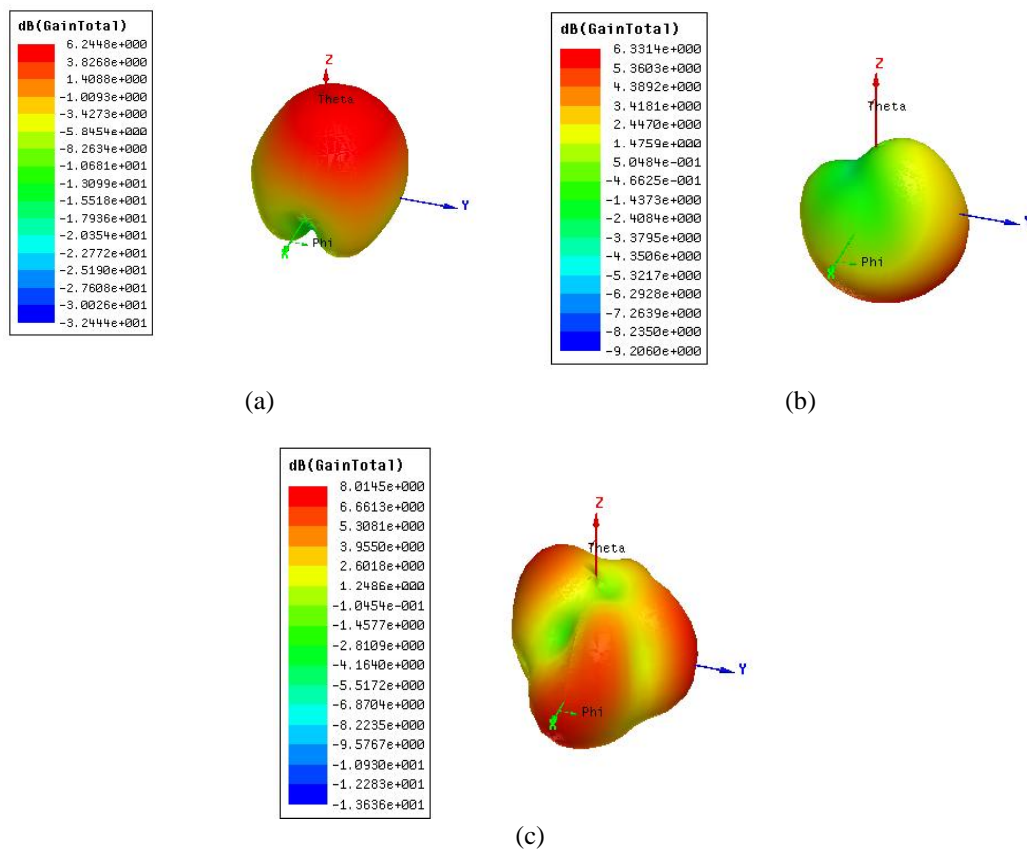


(a)



(b)



(c)

Figure 7. Gain of proposed antenna at different frequencies; (a) gain at 3.52 GHz, (b) gain at 7.5 GHz, and (c) gain at 9.72 GHz

When considering the azimuth and elevation angles of the antenna, the strength of the radio waves flowing from the antenna in different directions is stated to as the radiation pattern. Every antenna should have zero near end radiation and a fan-shaped radiation pattern at the far end. The radiation pattern for the frequencies of 3.52 GHz, 7.5 GHz, and 9.72 GHz at ϕ=0 and ϕ=90 degrees is shown in Figures 8(a)-(c) respectively which has been examined by the HFSS software. The power is carried to the far end of the specified antenna using azimuth and elevation angle.



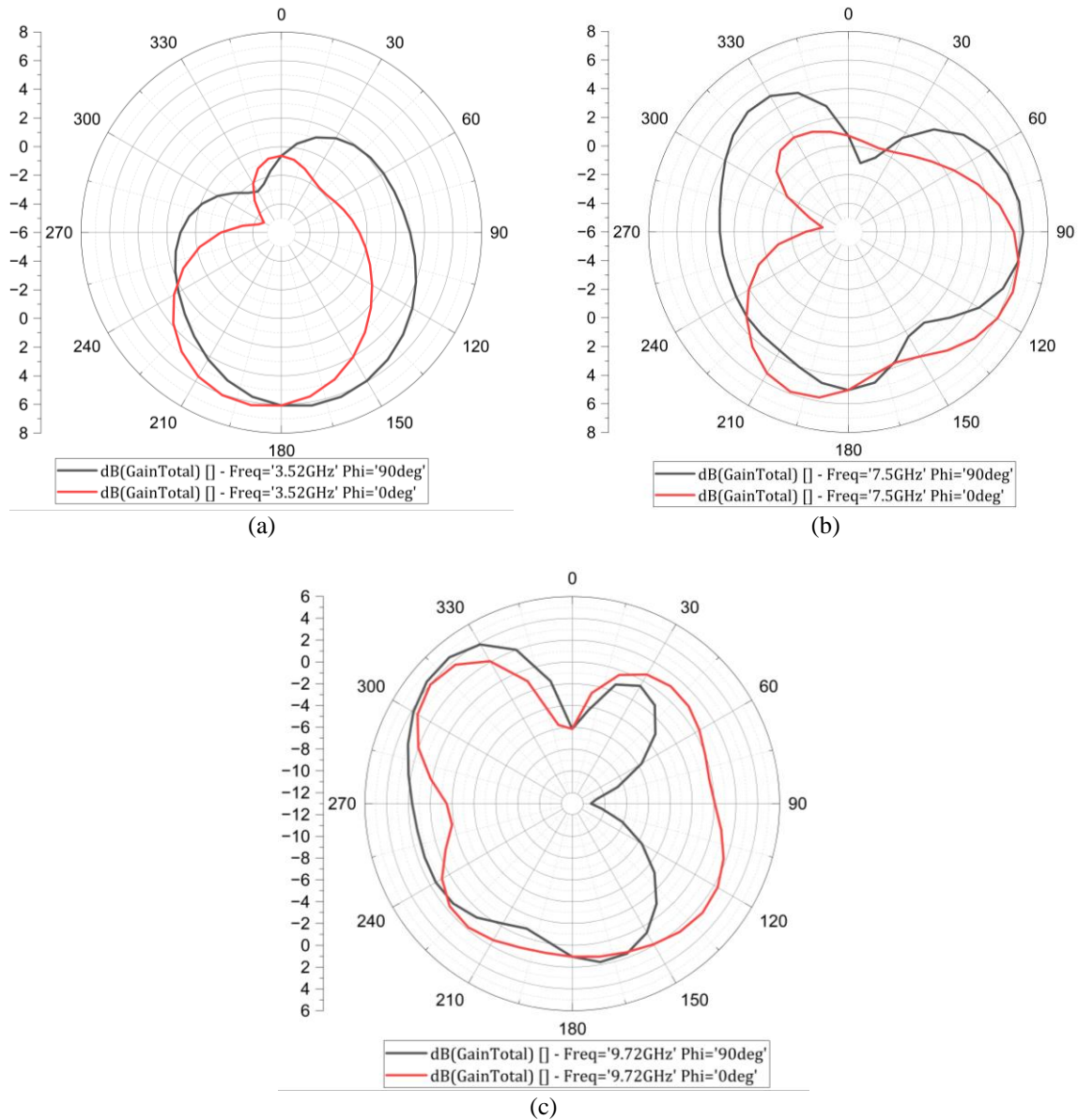(a)                                        (b)



(c)

Figure 8. Radiation pattern; (a) at 3.52 GHz, (b) at 7.5 GHz, and (c) at 9.72 GHz

Figure 9 displays the simulated distribution of surface current on patch antenna with C-CSRR, Figure 9(a) shows the spread at 3.52 GHz, Figure 9(b) shows at 7.5 GHz, and Figure 9(c) shows at 9.72 GHz, respectively. The distribution of surface current shown in the image highlights the performance benefits introduced by integrating a CSRR on the antenna structure. On the left side of the image, the high current density (indicated by red and orange) around the feedline and the coupling region confirms efficient excitation of the antenna. On the right, the strong localization of surface current around the CSRR slot confirms its resonance at the designed frequency. This behavior demonstrates the CSRR's role in concentrating electromagnetic energy, effectively adding distributed capacitance and inductance to the structure. As a result of this, the antenna achieves miniaturization by operating at lower frequencies without

increasing physical size. Additionally, the presence of the CSRR helps enhance bandwidth and suppress undesired frequencies, acting as a notch or filtering element. Overall, the surface current pattern verifies that the CSRR contributes to improved radiation control, resonance sharpness, and compact design.
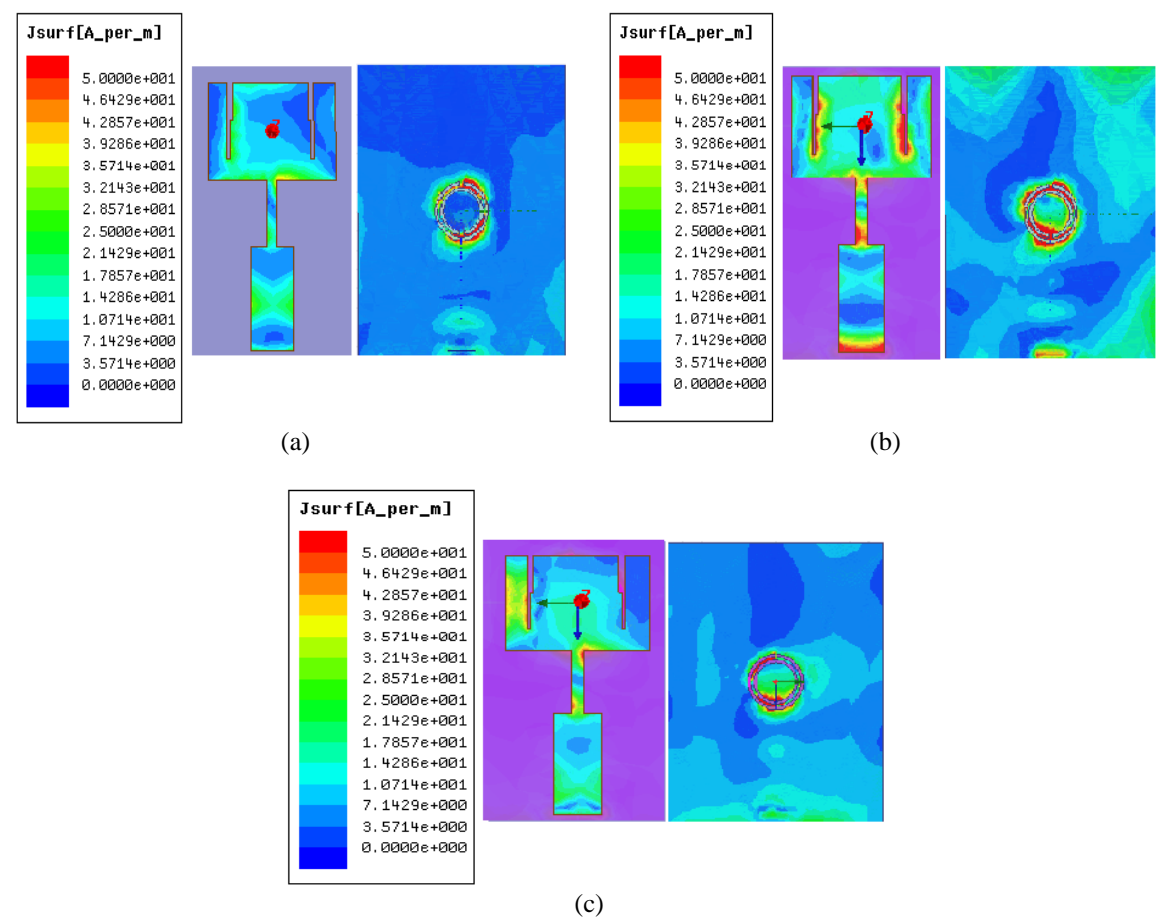


(a)



(b)



(c)

Figure 9. Surface current distribution on patch and ground plane; (a) surface current at 3.52 GHz, (b) surface current at 7.5 GHz, and (c) surface current 9.72 GHz

The suggested designs are simulated, then implemented, and then evaluated using a standard testing environment. This results in exact and improved tested values that demonstrate no loss when compared to simulated results. Table 2 exhibits the comparative outcomes of the recommended antenna's operation and Figure 10 illustrates the experimental setup for the measurements of different parameters of fabricated antennas; Figure 11 provides the front and back views of the fabricated antennas. In the same way, Figure 12 represents the tested results of the intended antennas.

Table 2. Comparison between conventional antenna and proposed antennas

| Developed antenna | Resonant frequency (GHz) | Return loss (dB) | Bandwidth (MHz) | Gain (dB) | Resonant frequency (GHz) | Return loss (dB) | Bandwidth (MHz) |
|---|---|---|---|---|---|---|---|
| | Simulated | Measured | Simulated | Measured | Simulated | Measured | Simulated |
| Conventional | 9.8 | 9.68 | -25.86 | -27.07 | 610 | 505 | 2.2 |
| Antenna with | 3.5 | 3.52 | -20.85 | -13.54 | 105 | 100 | 6.24 |
| CCSRR | 7.5 | 7.58 | -21.06 | -28.41 | 205 | 240 | 6.33 |
| | 9.7 | 8.2 | -27.92 | -21.07 | 437 | 400 | 8.014 |
| Antenna with | 3.5 | 3.5 | -24.13 | -13.23 | 110 | 90 | 2.13 |
| CCSRR and | 7.18 | 7.5 | -21.86 | -16.32 | 161 | 100 | 2.17 |
| slot | 8.49 | 8.8 | -30.87 | -30.26 | 120 | 330 | 2.95 |
| | 9.71 | 9.32 | -23.41 | -36.75 | 450 | 450 | 2.04 |

Figure 10. Experimental setup
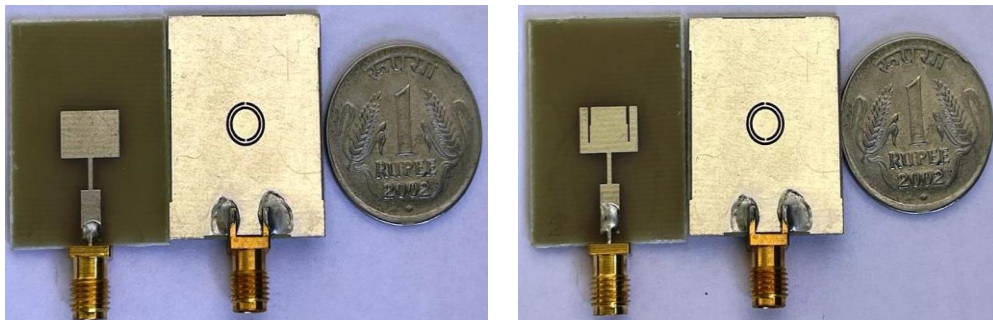


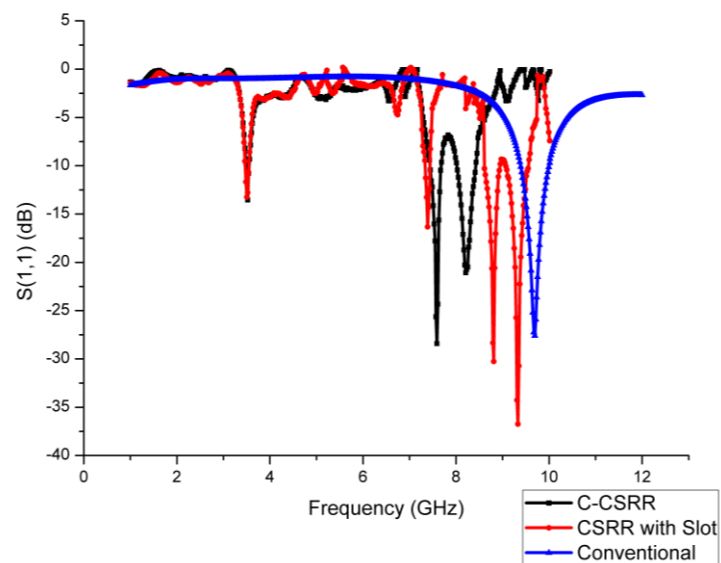Figure 11. The manufactured antennas' top and bottom views



Figure 12. Tested results of fabricated antennas

## 4.    COMPARISON WITH OTHER WORK

Table 3 summarizes the performance of our recommended Metamaterial antenna in comparison to various previously reported efforts. The works are listed according to a several parameters, among them are antenna's size, frequency range, bandwidth, and gain. The comparative procedure indicates that the suggested metamaterial antenna has certain exceptional qualities, including high gain, bandwidth, and return loss.

Table 3. Comparison with previous work

| Ref. number | Dimensions (mm×mm) | Resonant frequency (GHz) | Bandwidth | Gain | Radiation efficiency (%) |
|---|---|---|---|---|---|
| [2] | 45×45 | 2.45, 2.86, 6.19 | 180, 150, 420 | 3.16 | 74.99 |
| [5] | 30×30 | 2.4, 4.64 | 180, 2400 | 4.6 | 92 |
| [8] | 25×25 | 2.4, 5.2, 7.4, 8.2 | 220, 90, 110,100 | 1.22 | 90 |
| [13] | 40×30 | 2.4, 3.5 | 750, 110 | 1.26 | 70 |
| [19] | 30×30 | 5.26, 9.11 | 510, 900 | 5.3 | 96.88 |
| [23] | 70×63 | 3.1, 5.0 | 560, 950 | 4.63 | 92 |
| Proposed | 30.19×23.3 | 3.5, 7.5, 8.8, 9.32 | 110, 161, 120, 450 | 8.014 | 94.22 |

This antenna employs C-CSRRs, a kind of metamaterial design. Each C-CSRR slot introduces a new resonant frequency due to its unique inductive-capacitive resonance. By adjusting the number and dimensions of C-CSRRs (N=1, 2, or 3), the antenna supports multiple pass bands, each linked to a distinct resonance. Hence the proposed antenna outperforms others by leveraging metamaterial C-CSRRs to achieve multiband resonance, efficient radiation, and high gain within a significantly miniaturized footprint through enhanced electromagnetic field confinement and precise impedance control.

## 5. CONCLUSION

The proposed antennas have a few benefits, including a small size and support for a variety of applications in multiband frequencies. At all resonant frequencies, it is observed that the planned antenna has a gain of more than 6 dB. The antenna is perfect for 5G sub-6 GHz bands and other wireless technologies since it supports many frequency bands, such as 3.5 GHz permits incorporation into smart infrastructure, internet of things (IoT) devices, and small mobile devices. Miniaturization and multiband operation make it suitable for IoT sensors and edge devices that need to connect across various frequency bands. It can also be used in radar systems, secure communications, and remote command units where multiband, stealthy, and compact antennas are required. Based on the research, the developed antenna outperformed previous antenna designs in terms of gain and efficiency while using less dimensions. This is accomplished by modifying the current design and putting new methods into practice.

While the antenna resonates at multiple frequencies, the bandwidth at certain bands may be narrow, potentially limiting data throughput and making the system sensitive to frequency shifts. Future work will focus on integrating DGS techniques to enhance bandwidth.

## FUNDING INFORMATION

## AUTHOR CONTRIBUTIONS STATEMENT

This journal uses the Contributor Roles Taxonomy (CRediT) to recognize individual author contributions, reduce authorship disputes, and facilitate collaboration.

| Name of Author | C | M | So | Va | Fo | I | R | D | O | E | Vi | Su | P | Fu |
|---|---|---|---|---|---|---|---|---|---|---|---|---|---|---|
| Harshavardhan Reddy | ✓ | ✓ | ✓ | ✓ | ✓ | ✓ | | ✓ | ✓ | ✓ | ✓ | ✓ | ✓ | ✓ |
| Rajendra R. Patil | | | ✓ | | | ✓ | ✓ | ✓ | ✓ | ✓ | ✓ | ✓ | | |

| | | | | | |
|---|---|---|---|---|---|
| C | : | **C**onceptualization | I | : | **I**nvestigation |
| M | : | **M**ethodology | R | : | **R**esources |
| So | : | **So**ftware | D | : | **D**ata Curation |
| Va | : | **Va**lidation | O | : | Writing - **O**riginal Draft |
| Fo | : | **Fo**rmal analysis | E | : | Writing - Review & **E**diting |

| | | |
|---|---|---|
| Vi | : | **Vi**sualization |
| Su | : | **Su**pervision |
| P | : | **P**roject administration |
| Fu | : | **Fu**nding acquisition |

## CONFLICT OF INTEREST STATEMENT

Authors state that there is no conflict of interest.

## INFORMED CONSENT

We have informed and obtained consent from all individuals included in this study.

## DATA AVAILABILITY

Data availability is not applicable to this paper as no new data were created or analyzed in this study.

## REFERENCES

[1]    V. G. Veselago, "The electrodynamics of substances with simultaneously negative values of "ε, and μ"," *Soviet Physics Uspekhi*, vol. 10, no. 4, pp. 509–514, 1968.

[2]    M. Aminu-Baba *et al.*, "A compact triband microstrip antenna utilizing hexagonal CSRR for wireless communication systems," *Bulletin of Electrical Engineering and Informatics*, vol. 9, no. 5, pp. 1916–1923, Oct. 2020, doi: 10.11591/eei.v9i5.2191.

[3]    R. S. Daniel, R. Pandeeswari, and S. Raghavan, "A miniaturized printed monopole antenna loaded with hexagonal complementary split ring resonators for multiband operations," *International Journal of RF and Microwave Computer-Aided Engineering*, vol. 28, no. 7, pp. 1–8, 2018, doi: 10.1002/mmce.21401.

[4]    P. Manikandan, P. Sivakumar, and N. Rajini, "Multi-band Antenna with CSRR Loaded Ground Plane and Stubs Incorporated Patch for WiMAX/WLAN Applications," *Pertanika Journal of Science and Technology*, vol. 30, no. 1, pp. 35–52, Dec. 2022, doi: 10.47836/PJST.30.1.03.

[5]    B. Murugeshwari, R. S. Daniel, and S. Raghavan, "A compact dual band antenna based on metamaterial-inspired split ring structure and hexagonal complementary split-ring resonator for ISM/WiMAX/WLAN applications," *Applied Physics A: Materials Science and Processing*, vol. 125, no. 9, pp. 1–8, Sep. 2019, doi: 10.1007/s00339-019-2925-x.

[6]    A. K. Vallappil, B. A. Khawaja, M. K. A. Rahim, M. N. Iqbal, and H. T. Chattha, "Metamaterial-Inspired Electrically Compact Triangular Antennas Loaded with CSRR and 3×3 Cross-Slots for 5G Indoor Distributed Antenna Systems," *Micromachines*, vol. 13, no. 2, pp. 1–16, Jan. 2022, doi: 10.3390/mi13020198.

[7]    J. Yeo and J. I. Lee, "Design of a high-sensitivity microstrip patch sensor antenna loaded with a defected ground structure based on a complementary split ring resonator," *Sensors*, vol. 20, no. 24, pp. 1–18, Dec. 2020, doi: 10.3390/s20247064.

[8]    R. Rajkumar and U. K. Kommuri, "A Triangular Complementary Split Ring Resonator Based Compact Metamaterial Antenna for Multiband Operation," *Wireless Personal Communications*, vol. 101, no. 2, pp. 1075–1089, Jul. 2018, doi: 10.1007/s11277-018-5749-7.

[9]    M. H. Reddy, D. Sheela, V. K. Parbot, and A. Sharma, "A compact metamaterial inspired UWB-MIMO fractal antenna with reduced mutual coupling," *Microsystem Technologies*, vol. 27, no. 5, pp. 1971–1983, May 2021, doi: 10.1007/s00542-020-05024-z.

[10]   G. Geetharamani and T. Aathmanesan, "Design of Metamaterial Antenna for 2.4 GHz WiFi Applications," *Wireless Personal Communications*, vol. 113, no. 4, pp. 2289–2300, Aug. 2020, doi: 10.1007/s11277-020-07324-z.

[11]   Saktioto *et al.*, "Improvement of low-profile microstrip antenna performance by hexagonal-shaped SRR structure with DNG metamaterial characteristic as UWB application," *Alexandria Engineering Journal*, vol. 61, no. 6, pp. 4241–4252, Jun. 2022, doi: 10.1016/j.aej.2021.09.048.

[12]   R. K. Saraswat and M. Kumar, "Design and Implementation of a Multiband Metamaterial-Loaded Reconfigurable Antenna for Wireless Applications," *International Journal of Antennas and Propagation*, pp. 1–21, Dec. 2021, doi: 10.1155/2021/3888563.

[13]   R. Sahoo and D. Vakula, "Compact metamaterial inspired conformal dual-band antenna loaded with meander lines and fractal shaped inductor for Wi-Fi and WiMAX applications," *IET Microwaves, Antennas and Propagation*, vol. 13, no. 13, pp. 2349–2359, Oct. 2019, doi: 10.1049/iet-map.2018.6008.

[14]   S. S. Al-Bawri, M. T. Islam, T. Shabbir, G. Muhammad, M. D. Shabiul Islam, and H. Y. Wong, "Hexagonal shaped near zero index (NZI) metamaterial based MIMO antenna for millimeter-wave application," *IEEE Access*, vol. 8, pp. 181003–181013, 2020, doi: 10.1109/ACCESS.2020.3028377.

[15]   P. Kaur, S. Bansal, and N. Kumar, "SRR metamaterial-based broadband patch antenna for wireless communications," *Journal of Engineering and Applied Science*, vol. 69, no. 1, pp. 1–12, Dec. 2022, doi: 10.1186/s44147-022-00103-6.

[16]   W. Cao, Y. Xiang, B. Zhang, A. Liu, T. Yu, and D. Guo, "A low-cost compact patch antenna with beam steering based on CSRR-loaded ground," *IEEE Antennas and Wireless Propagation Letters*, vol. 10, pp. 1520–1523, 2011, doi: 10.1109/LAWP.2011.2181316.

[17]   S. Manoharan, P. Ramasamy, and R. Singaravelu, "A quad-band fractal antenna with metamaterial resonator-backed ground for sub-6 GHz, C and X band applications," *Applied Physics A: Materials Science and Processing*, vol. 127, no. 9, p. 703, Sep. 2021, doi: 10.1007/s00339-021-04862-6.

[18]   L. Su, J. Naqui, J. Mata-Contreras, and F. Martin, "Modeling and Applications of Metamaterial Transmission Lines Loaded with Pairs of Coupled Complementary Split-Ring Resonators (CSRRs)," *IEEE Antennas and Wireless Propagation Letters*, vol. 15, pp. 154–157, 2016, doi: 10.1109/LAWP.2015.2435656.

[19]   L. He, S. Yi, and H. Yang, "High-efficiency compact SRR–CSRR–SIW antenna based on CRLH-TL," *Journal of Electromagnetic Waves and Applications*, vol. 36, no. 1, pp. 69–82, Jan. 2022, doi: 10.1080/09205071.2021.1957025.

[20]   N. R. Kumar, P. D. Sathya, S. K. A. Rahim, M. Z. M. Nor, A. Alomainy, and A. A. Eteng, "Compact tri-band microstrip patch antenna using complementary split ring resonator structure," *Applied Computational Electromagnetics Society Journal*, vol. 36, no. 3, pp. 346–353, Apr. 2021, doi: 10.47037/2020.ACES.J.360314.

[21]   D. Allin Joe and T. Krishnan, "A Triband Compact Antenna for Wireless Applications," *International Journal of Antennas and Propagation*, pp. 1–13, Sep. 2023, doi: 10.1155/2023/5344999.

[22]   M. S. Rao and P. I. Basarkod, "A novel complementary slotted split ring resonator loaded truncated arc patch antenna with enhanced performance," *Progress In Electromagnetics Research C*, vol. 101, pp. 203–218, 2020, doi: 10.2528/PIERC20031003.

[23]   C. Pochaiya, S. Chandhaket, P. Leekul, J. Mearnchu, T. Tantisopharak, and T. Limpiti, "Bandwidth enhancement of dual-band bi-directional microstrip antenna using complementary split ring resonator with defected structure for 3/5 GHz applications," *International Journal of Electrical and Computer Engineering*, vol. 12, no. 2, pp. 1683–1694, Apr. 2022, doi: 10.11591/ijece.v12i2.pp1683-1694.

[24]   M. Shobana, "CSRR inspired antenna using artificial neural network for sub 6 GHz 5G applications," *Alexandria Engineering Journal*, vol. 77, pp. 351–367, Aug. 2023, doi: 10.1016/j.aej.2023.06.085.

[25]   C. J. M. Andrews, A. S. K. Narayanan, and A. Marazhchal Sunil, "Compact Metamaterial based Antenna for 5G Applications," *Results in Engineering*, vol. 24, pp. 1–8, Dec. 2024, doi: 10.1016/j.rineng.2024.103269.

## BIOGRAPHIES OF AUTHORS

**Harshavardhan Reddy** received Bachelor of Engineering in Electronics and Communication Engineering from Visvesvaraya Technological University (VTU) Belagavi, Karnataka, India in 2008 and received Master of Technology in Communication Systems PDA autonomous institution affiliated by Visveswaraiah Technological University in 2012. He is working as Assistant Professor at Sharnbasva University Kalaburagi, Karnataka, India. His main research interests are microstrip patch antennas and wireless communication. He can be contacted at email: harshareddy86@gmail.com.

**Dr. Rajendra R. Patil** received Bachelor of Engineering in Electronics and Communication Engineering, PDAEC, Kalaburagi in 1991, Master of Technology in Power Electronics, PDAEC, Kalaburagi in 2006 and Ph.D. in Applied Electronics (Microwave), Gulbarga University, Kalaburagi in 2016. He is working as Professor and HOD at GSSS IET for Women, Mysuru, India. His main research interests are microwave engineering, wireless communication, and embedded systems. There are more than 50 publications in journals, conference proceedings and book chapters. He can be contacted at email: rajendra.nano@gmail.com.